PII: S0272-8842(96)00011-9

Ceramics International 23 (1997) 191–196

0272-8842/97 $17.00+.00

Synthesis and Characterisation of Lead Magnesium Niobate Having Exceptionally High Dielectric Constant

S. M. Gupta,[a] C. S. Harendranath[b] & A. R. Kulkarni[a]

[a]Department of Metallurgical Engineering and Materials Science, Indian Institute of Technology, Bombay 400 076, India
[b]Regional Sophisticated Instrumentation Centre, Indian Institute of Technology, Bombay 400 076, India

(Received 12 June 1995; accepted 23 November 1995)

Abstract: Exceptionally high dielectric constant, $\approx$28,000 (1 kHz) at T_c (−18 °C) has been achieved in stoichiometric lead magnesium niobate (PMN) ceramics prepared by partial oxalate route. Sintering at 1300 °C for 2 h in closed alumina crucible resulted in a highly dense PMN sample. Dielectric measurements with frequency showed a typical relaxor behaviour. Microstructure investigation along with electron probe microanalysis (EPMA) provide interesting clues to the observed material behaviour. Apart from grain size and density, lead oxide distribution controls the dielectric properties. © 1997 Elsevier Science Limited and Techna S.r.l. All rights reserved

1 INTRODUCTION

The perovskite relaxor ferroelectric lead magnesium niobate [$Pb(Mg_{1/3}Nb_{2/3})O_3$] exhibits high dielectric constant, low sintering temperature, and broad dielectric maxima at T_c. Synthesis of this family of compounds has, however, been found to be rather difficult because of the pyrochlore phase formation mainly from the loss of PbO during sintering, irrespective of the methods used.[1–10] The stable pyrochlore phase in PMN is also known to reduce the dielectric constant of the material.[11] Initial efforts with the development of PMN ceramics were directed towards minimising this pyrochlore phase. Addition of excess PbO has been the most widely used method to minimise the pyrochlore phase. These reports, however, do not discuss the effect of excess PbO on the dielectric behaviour of PMN. The logarithmic law for a mixture of dielectrics suggests that the lower dielectric constant of PbO ($\approx$20) will have a higher influence on the permittivity of PMN than that of pyrochlore phase, which has a dielectric constant of $\approx$120. This means that 2% free PbO at the grain boundary will reduce the dielectric constant of PMN more severely than 2% pyrochlore phase. The role of excess PbO on the dielectric properties of PMN has recently been studied.[12,13] It was concluded that excess PbO decreases the dielectric behaviour of PMN more severely than the pyrochlore phase. The decrease of the dielectric constant by excess PbO is attributed to an increase of the PbO layer at the grain boundary. Generally, in lead based relaxor materials, the excess or unreacted PbO segregates at the grain boundary and leads to a reduction in dielectric constant. This reduction in dielectric constant has been explained on the basis of "grain volume effect" on the high permittivity of PMN grain.[14] Thus PMN samples should be free of unreacted PbO at the grain boundary. The thickness of PbO layer at the grain boundary decreases with increase in the sintering temperature or increase in the grain size. A PbO grain boundary layer for stoichiometric PMN has been calculated to be 1.2 nm thick[13] when sintered at 1200 °C for 1 h. The purpose of this work has been to reduce the thickness of this PbO layer at the grain boundary in order to achieve very high dielectric constant. To achieve this, the sample was sintered at 1300 °C for 2 h in a closed alumina crucible. This sintering temperature was chosen to get the maximum grain size as above this firing temperature the PMN disks were completely melted when the sintering time was kept constant. Electron probe microanalysis, along with scanning electron microscopy, has been used to study the PbO distribution over grain and grain boundaries. The stoichiometric PMN was prepared by partial oxalate and columbite route. The EPMA study of these samples are compared with PMN sample containing 2 wt% excess PbO and fired at 900 °C in closed alumina crucible. The results of electron probe microanalysis, phase analysis, dielectric properties, microstructure and physical properties of stoichiometric PMN have been discussed further.

2 EXPERIMENTAL

Starting powders of niobium oxide (Nb_2O_5) (special pure grade, Aldrich, USA), magnesium carbonate ($MgCO_3$) and lead nitrate ($Pb(NO_3)_2$) (reagent grade, BDH, UK) were used in as received condition. The lead solution was prepared by dissolving $Pb(NO_3)_2$ in double distilled water. The flow diagram of the partial oxalate route is shown in Fig. 1. The columbite precursor was prepared by mixing $MgCO_3$ and Nb_2O_5 in methanol for 1 h using automated agate mortar and pestle (Retsch mortar Grinder, Type RMO, W. Germany) and, after drying, fired at 1100 °C for 4 h. The procedure was repeated twice to ensure complete reaction. The formation of single phase magnesium niobate was confirmed by XRD. The precursor was sprinkled in oxalic acid solution, stirred for 1 h and then lead nitrate solution was added dropwise. In the reaction that follows, lead from the nitrate solution precipitates as lead oxalate and has been assumed to coat[15] the calcined powders giving a homogeneous mixture. These precipitates were washed several times with distilled water. The powder was pre-sintered at 800 °C.

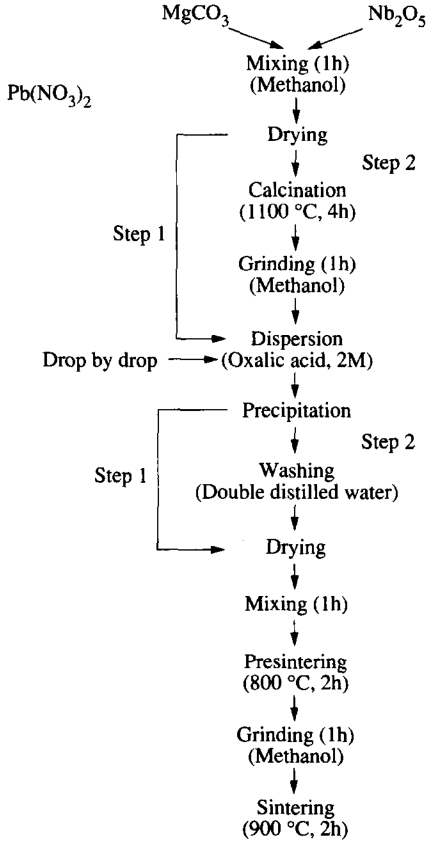

Fig. 1. Flow diagram of partial oxalate route for PMN preparation.

Lead magnesium niobate was also prepared by columbite method in which PbO (Aldrich, 99.9%) was mixed, similarly as described for the partial oxalate method, with columbite precursor and pre-sintered at 800 °C.

Pre-sintered powders were crushed and mixed for 1 h in methanol using automated agate mortar and pestle. The mixed powders were pressed as disks (15 mm diameter, 2–3 mm thick) and buried in MgO powder and sintered at 1300 °C for 2 h in a closed alumina crucible at a rate of 3 °C per min. The pellets were fired in a closed alumina crucible to minimise the lead oxide loss from the pellets. Similarly, PMN with 2 wt% excess PbO sample was prepared by partial oxalate route and was fired at 900 °C.

The phase analysis of the pre-sintered and sintered ceramic was carried out using X-ray diffraction (Jeol DL 5400, Japan) with Cu Kα radiation of wavelength = 1.5406 Å. For dielectric measurements, the sintered disks were polished on different grades of emery paper. Electrical contacts on the parallel surfaces were facilitated by gold sputtering (Edward 360, UK). In addition, the gold layer was covered with room temperature curable silver paint (Eltech, Bangalore, India) to improve the contacts. Dielectric properties were measured with Impedance Gain Phase Analyser (Schlumberger, number SI 1260, UK) at four different frequencies (0.1, 1, 10, 50 kHz) with 1 V/rms, during cooling over a range of temperatures (−30 °C to 80 °C). The temperature was controlled to ± 1 °C. Microstructure study and electron probe microanalysis was carried out on graphite coated fracture surface of PMN material using a CAMECA SU SEM-Probe Analytical Scanning Electron Microscope (France). Quantitative X-ray microanalysis has been carried out using an inclined wavelength dispersive X-ray spectrometer.

3 RESULTS AND DISCUSSION

3.1 *Phase analysis*

The XRD pattern of the sintered samples prepared by partial oxalate and columbite methods are shown in Fig. 2. The amount of pyrochlore phase

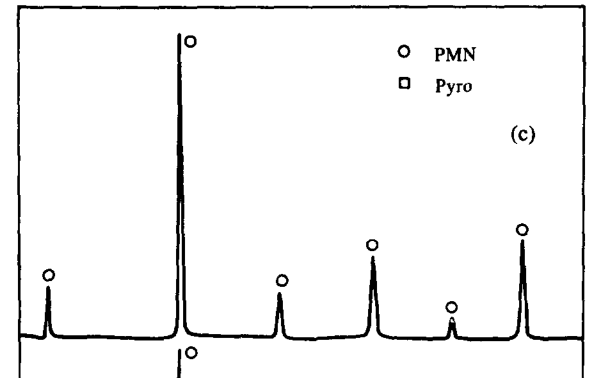

Fig. 2. X-ray diffraction pattern of the PMN samples prepared by partial oxalate and columbite routes: (a) [PMN(2P900)], (b) [PMN(P1300)] and (c) [PMN(C1300)]. The material was soaked for 2 h at each sintering temperature.

present in each sample is calculated from the relative intensities of the major X-ray reflection for the pyrochlore and the perovskite phase as reported in the literature.[2]

$$\text{Pyrochlore phase} = \frac{I_{\text{pyro}}}{I_{\text{pyro}} + I_{\text{PMN}}} \times 100 \qquad (1)$$

where I_{pyro} refers to the (222) pyrochlore peak and I_{PMN} refers to (110) perovskite peak. The percentage of perovskite phase and pyrochlore phase present in the sintered samples, along with sample codes, physical properties and dielectric properties, are given in Table 1.

It may be noticed that both the sintered specimens [PMN(P1300)] and [PMN(C1300)] show the formation of single phase PMN, whereas nearly 6.5% pyrochlore phase has been found in [PMN(2P900)] sample. The presence of 6.5% pyrochlore phase in [PMN(2P900)] is attributed to low diffusivity of PbO at lower temperature.

3.2 Dielectric properties

The temperature dependence of the dielectric constant and dissipation factor at 1 kHz for [PMN(2P900)], [PMN(C1300)] and [PMN(P1300)] are compared in Fig. 3 (a) and (b), respectively. Both the specimens, [PMN(C1300)] and [PMN(P1300)], show a broad maximum for the dielectric constant and negligible dissipation factor (0.0025) at room temperature. The dissipation factor increases to approximately 0.04 at the Curie temperature (T_c). The dielectric constant ($K_{\max}$) and loss maxima shift towards a higher temperature (T_c) with increasing frequency, i.e. a typical relaxor behaviour. In contrast, the [PMN(2P900)] sample does not show good relaxor characteristics as may be seen from Fig. 3(a). The reason for this type of dielectric behaviour may be the non-uniform distribution of PbO along the grain and grain boundaries which is supported by microstructure study discussed later. From Fig. 3 it is clear that the maxima in the dielectric constant vs temperature plots increase remarkably with increase in the sintering temperature. The most important feature of this study is the dielectric constant ($K_{\max}$) value for [PMN(P1300)] sample that is shown in Fig. 3(b). The maximum dielectric constant of [PMN(P1300)] at 1 kHz is 28000, whereas for [PMN(C1300)] it is 24000. These values are higher than those reported in the literature so far. The possible reasons for this high value may be uniform distribution of lead oxide over grain, which means there is no inactive "shell" like region over the "core" region of PMN

Table 1. Phase analysis, physical and dielectric properties for PMN prepared by partial oxalate route and columbite method

	Phase		Physical		Dielectric		
Samples	PMN	PYRO	Density*	Porosity	$K_{\max}$$	T_c#	Tanδ$
PMN(2P900)	93.6%	6.4%	6.58	18.5%	2600	+3	0.041
PMN(P1300)	100.0%	0.0%	7.79	0.1%	28450	−19	0.044
PMN(C1300)	99.0%	1.0%	7.78	0.6%	24300	−18	0.038

*Values are in gm/cc.
#Temperature in 1 °C.
$Values are at 1 kHz.

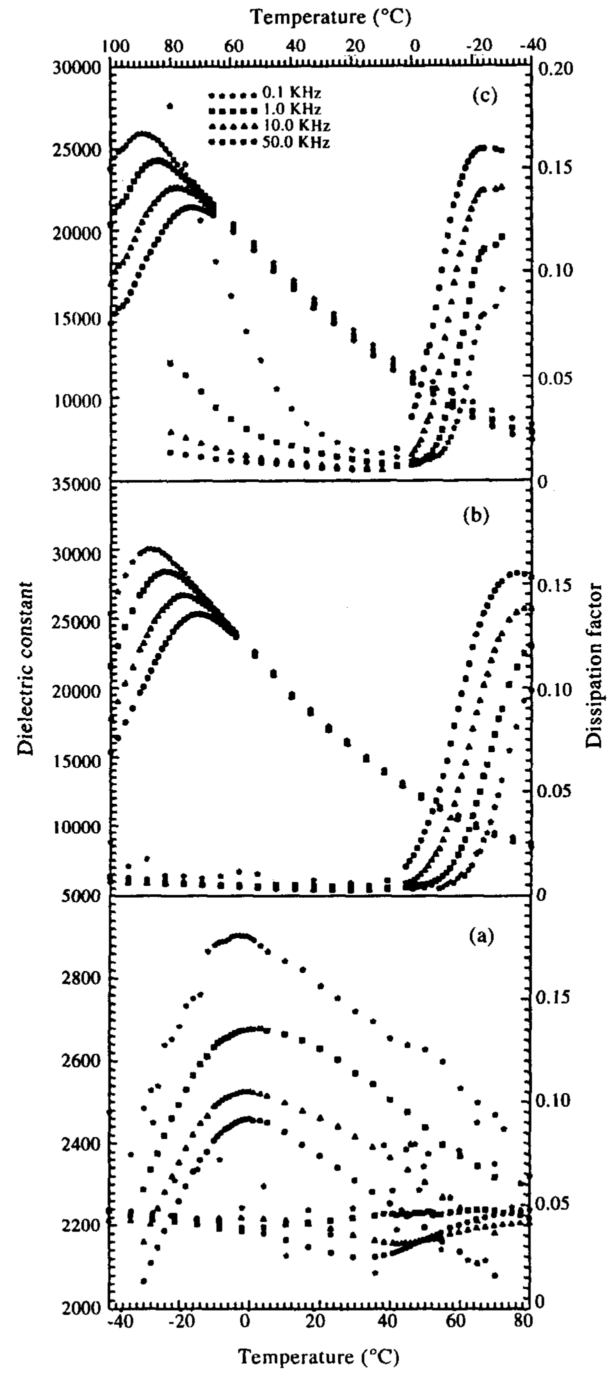

Fig. 3. Comparison of (a) dielectric constant [1kHz] and (b) dissipation factor [1kHz] vs temperature at four fixed frequencies for (a) [PMN(2P900)], (b) [PMN(P1300)] and (c) [PMN(C1300)]

grain.[16] According to Viehland *et al.*[17] each grain has two regions, a core region and surrounding this an inactive low polarizable region, i.e. shell region. The dielectric constant of the inactive "shell" region is 300 and the thickness of this region was assumed to be 15 nm. The shell region decreases with increase in sintering temperature. Thus, it may be possible to reduce the shell region further by increasing the sintering temperature and avoiding any lead oxide loss from the sample. It seems for PMN(C1300) and PMN(P1300) the inactive shell region or the thickness of PbO layer in grain boundary is negligible. Hence, a very high value of dielectric constant is achieved in these samples.

The density and porosity of the compacts are determined using Archimedes principle[18] and are reported in Table 1. It may be noted that density of the sintered samples in [PMN(C1300)] and [PMN(P1300)] are nearly the same as the theoretical density of PMN. The dielectric constant ($K_{\max}$) is corrected for density of the samples[19] as reported in literature.

$$K_{\text{corrected}} = \frac{K_{\text{observed}} \times (2 + V_2)}{2(1 - V_2)} \tag{2}$$

where V_2 is the volume fraction of porosity present in the sample. The observed and corrected dielectric constant ($K_{\max}$) values are also reported in Table 2.

3.3 Microstructure

The scanning electron micrographs of fractured surfaces of the compacts fired at 900 and 1300 °C are shown in Fig. 4(a)–(c). All the samples show predominantly intergranular fracture. The average grain size of [PMN(C1300)] and [PMN(P1300)] samples is between 6–7 μm and grains are tightly packed which is in line with porosity measurements. However, the average grain size of [PMN(2P900)] sample is less than 1 μm and the porosity is very high compared with that of [PMN(C1300)] and [PMN(P1300)] samples.

Table 2. Porosity correction on the dielectric constant and average grain size for PMN prepared by partial oxalate and columbite route

Sample no.	Samples	K_{observed} (1 kHz)	$K_{\text{corrected}}$* (1 kHz)	Grain size (μm)
1	PMN(2P900)	2600	3150	≈<1.0
2	PMN(P1300)	28450	28540	≈6–7
3	PMN(C1300)	24300	26700	≈6–7

$$*K_{\text{corrected}} = \frac{K_{\text{observed}} \times (2 + V_2)}{2(1 - V_2)}$$

Electron probe microanalysis studies were carried out on PMN grains to determine the composition. Three different points were taken on the grain for this study. It may be noticed that in [PMN(2P900)] sample the EPMA study was carried out considering a number of grains because of its small grain size, whereas in [PMN(C1300)] and [PMN(P1300)] samples the grain at which EPMA study was carried out are marked "X" in Fig. 4. The average composition of [PMN(C1300)] is [$Pb_{0.962}Mg_{0.325}Nb_{0.635}O_{3.122}$], and for [PMN(P1300)] is [$Pb_{0.978}Mg_{0.236}Nb_{0.583}O_{2.284}$].

Microprobe X-ray line profile analysis over grains and grain boundaries was carried out for the lead oxide variation. The scanned micrographs of [PMN(2P900)], [PMN(C1300)] and [PMN(P1300)] samples are shown in Fig. 5(a)–(c), respectively. It can be noted from Fig. 5(a) that the lead distribution

Fig. 4. Scanning electron microstructure of (a) [PMN(2P900)], (b) [PMN(P1300)] and (c) [PMN(C1300)].; calcined at 800 °C for 2 h.

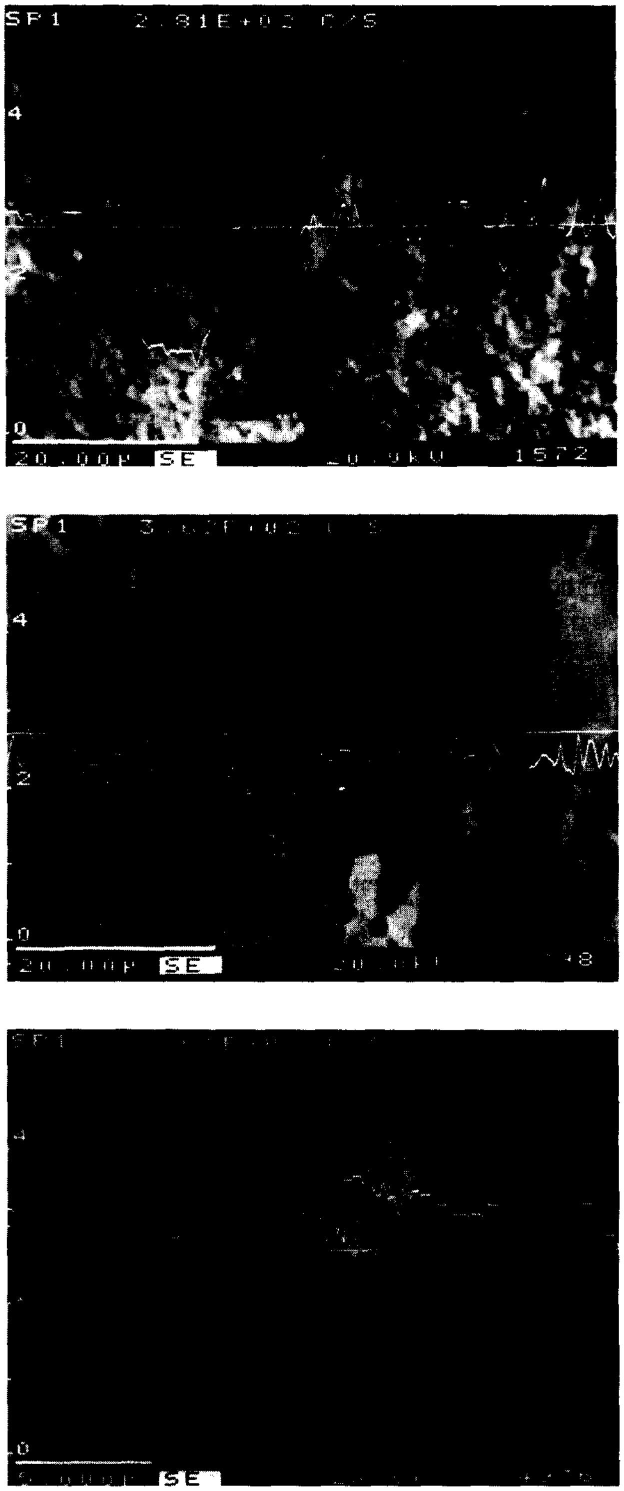

Fig. 5. Microprobe X-ray line profile analysis of lead on (a) [PMN(2P900)], (b) [PMN(P1300)] and (c) [PMN(C1300)].

is not uniform, whereas there is no lead enrichment or depletion region in Fig. 5(b) and (c) for [PMN(C1300)] and [PMN(P1300)] samples. A sharp dip in Fig. 5(a) indicates a lead depleted region in [PMN(2P900)] sample.

In the present case, the exceptionally high dielectric constant in [PMN(C1300)] and [PMN(P1300)] is attributed to very large grain size, high density and uniform distribution of PbO over grain and grain boundaries or, in other words, the absence of the PbO layer at the grain boundary. Thus, it may stated that the exceptionally high dielectric constant is on account of the combined effect of (1) high grain size, (2) uniform lead distribution and (3) very high density.

4 CONCLUSION

Exceptionally high dielectric constant is achieved in lead magnesium niobate prepared by partial oxalate route and columbite method. The PMN samples, fired at 1300 °C in closed alumina crucible, show a very high density which is close to the theoretical density. Microstructure and EPMA studies reveal that grain size, lead distribution and absence of the PbO layer in grain boundary have a significant influence on the dielectric properties of the material.

REFERENCES

1. SWARTZ, S. L. & SHROUT, T. R., Fabrication of perovskite lead magnesium niobate. *Mater. Res. Bull.*, **17** (1982) 1245–1250.
2. LEJEUNE, M. & BOILOT, J. P., Optimisation of dielectric properties of lead magnesium niobate ceramics. *Am. Ceram. Soc. Bull.*, **64** (1984) 679–682.
3. LEJEUNE, M. & BOILOT, J. P., Low firing dielectric based on lead magnesium niobate. *Mater. Res. Bull.*, **20** (1985) 493–499.
4. GUHA, J. P. & ANDERSON, H. U., Preparation of perovskite $Pb(Mg_{1/3}Nb_{2/3})O_3$ using $Pb_3Nb_2O_8$ and MgO. *J. Am. Ceram. Soc.*, **69** (1986) C287–288.
5. CHAPUT, F., BOILOT, J. P., LEJEUNE, M., PAPIERNIK, R. & PFAIZGRAG, L. G., Low temperature route to lead magnesium niobate. *J. Am. Ceram. Soc.*, **72** (1989) 1355–1357.
6. KATAYAMA, K., ABE, M. & AKIBA, T., Preparation of $Pb(Mg_{1/3}Nb_{2/3})O_3$ powder by molten salt method. *Ceram. Int.*, **15** (1989) 289–295.
7. CHOY, J. H., YOO, J. S., KANG, S. G., HONG, S. T. & KIM, D. G., Ultrafine $Pb(Mg_{1/3}Nb_{2/3})O_3$ (PMN) powder synthesised from metal citrate gel by thermal shock method. *Mater. Res. Bull.*, **25** (1990) 283–291.
8. SHROUT, T. R., PAPET, P., KIM, S. & LEE, G. S., Conventionally prepared submicrometres lead based perovskite powders by reactive calcination. *J. Am. Ceram. Soc.*, **73** (1990) 1862–1867.
9. WATABNABE, A., HANEDA, H., MOSIYOSHI, Y., SHIRASHAKI, S., KURAMOTO, S. & YAMAMURA, A., Preparation of lead magnesium niobate by coprecipitation method. *J. Mater. Sci.*, **27** (1992) 1245–1249.
10. GUPTA, S. M. & KULKARNI, A. R., Synthesis of perovskite lead magnesium niobate using partial oxalate method. *Mater. Res. Bull.*, **28** (1993) 1295–1301.
11. SWARTZ, S. L. & SHROUT, T. R., Dielectric properties of pyrochlore lead magnesium niobate. *Mater. Res. Bull.*, **41** (1983) 663–667.
12. GUPTA, S. & KULKARNI, A. R., Effect of excess PbO on the dielectric properties of lead magnesium niobate synthesised by partial oxalate route. *J. Mater. Res.*, **10** (1995) 953–961.
13. WANG, H. C. & SCHULZE, W. A., The role of excess magnesium oxide or lead oxide in determining the microstructure and properties of lead magnesium niobate. *J. Am. Ceram. Soc.*, **73** (1990) 825–832.
14. SWARTZ, S. L., SHROUT, T. R., SCHULZE, W. A. & CROSS, L. E., Dielectric properties of lead magnesium niobate ceramics. *J. Am. Ceram. Soc.*, **67** (1984) 311–315.
15. OKAZAKI, K., Advanced technology in electroceramics in Japan. *Am. Ceram. Soc. Bull.*, **67** (1988) 1946–1949.
16. PAPET, P., DOUGHERTY, J. P. & SHROUT, T. R., Particle and grain size effects on the dielectric behaviour of the relaxor ferroelectric $Pb(Mg_{1/3}Nb_{2/3})O_3$. *J. Mater. Res.*, **5** (1990) 2902–2909.
17. VIEHLAND, D., JANG, S. J., WUTTIG, M. & CROSS, L. E., Freezing of the polarization fluctuation in lead magnesium niobate relaxors. *J. Appl. Phys.*, **120** (1991) 2916–2921.
18. ASTM Std, *1989 Annual Book of ASTM Standards*, Vol. 15.02, C373-88, P109-110. ASTM, 1916 Race Street, Philadelphia, PA, 1989, 19103–19118.
19. RUSHMAN, D. F. & STRIVENS, M. A., The permittivity of polycrystals of the perovskite type. *Proc. Phys. Soc.*, **59** (1947) 1011–1019.